


The heparan sulfate proteoglycan syndecan-1 regulates colon cancer stem cell function via a focal adhesion kinase—Wnt signaling axis

Sampath Kumar Katakam¹, Valeria Tria², Wey-Cheng Sim³, George W. Yip³, Stefano Molgora², Theodoros Karnavas^{4,5}, Eslam A. Elghonaimy^{6,*}, Paride Pelucchi², Eleonora Piscitelli², Sherif Abdelaziz Ibrahim⁶, Ileana Zucchi², Rolland Reinbold², Burkhard Greve⁷ and Martin Götte¹ 

1 Department of Gynecology and Obstetrics, Münster University Hospital, Germany

2 Istituto di Technologie Biomediche Consiglio Nazionale dell Ricerche, ITB-CNR, Segrate-Milano, Italy

3 Department of Anatomy, Yong Loo Lin School of Medicine, National University of Singapore, Singapore

4 Chromatin Dynamics Unit, Vita Salute San Raffaele University and Research Institute, Milan, Italy

5 Department of Neurosurgery, NYU Langone Medical Center, New York, NY, USA

6 Department of Zoology, Faculty of Science, Cairo University, Giza, Egypt

7 Department of Radiotherapy – Radiooncology, University Hospital Münster, Germany

Keywords

extracellular matrix; glycosaminoglycan; syndecans; tumor-initiating cells; xenograft

Correspondence

M. Götte, Department of Gynecology and Obstetrics, Münster University Hospital, Domagkstrasse 11, D-48149 Münster, Germany

Tel: +49-251-8356117

and

E-mail: mgotte@uni-muenster.de

B. Greve, Klinik für Strahlentherapie -

Radioonkologie-Universitätsklinikum

Münster, Albert-Schweitzer-Campus 1

Gebäude A1, D-48149 Münster, Germany

Tel: +49 251 8352537

E-mail: greveb@uni-muenster.de

Present address

*Department of Radiation Oncology, UT Southwestern Medical Center, Dallas, TX, 75390, USA

Burkhard Greve and Martin Götte contributed equally to this work

In colon cancer, downregulation of the transmembrane heparan sulfate proteoglycan syndecan-1 (Sdc-1) is associated with increased invasiveness, metastasis, and dedifferentiation. As Sdc-1 modulates signaling pathways relevant to stem cell function, we tested the hypothesis that it may regulate a tumor-initiating cell phenotype. Sdc-1 small-interfering RNA knockdown in the human colon cancer cell lines Caco2 and HT-29 resulted in an increased side population (SP), enhanced aldehyde dehydrogenase 1 activity, and higher expression of CD133, LGR5, EPCAM, NANOG, SRY (sex-determining region Y)-box 2, KLF2, and TCF4/TCF7L2. Sdc-1 knockdown enhanced sphere formation, cell viability, Matrigel invasiveness, and epithelial-to-mesenchymal transition-related gene expression. Sdc-1-depleted HT-29 xenograft growth was increased compared to controls. Decreased Sdc-1 expression was associated with an increased activation of β 1-integrins, focal adhesion kinase (FAK), and wingless-type (Wnt) signaling. Pharmacological FAK and Wnt inhibition blocked the enhanced stem cell phenotype and invasive growth. Sequential flow cytometric SP enrichment substantially enhanced the stem cell phenotype of Sdc-1-depleted cells, which showed increased resistance to doxorubicin chemotherapy and irradiation. In conclusion, Sdc-1 depletion cooperatively enhances activation of integrins and FAK, which then generates signals for increased invasiveness and cancer stem cell properties. Our findings may provide a novel concept to target a stemness-associated signaling axis as a therapeutic strategy to reduce metastatic spread and cancer recurrence.

Abbreviations

ALDH, aldehyde dehydrogenase; ARHGAP, Rho GTPase-activating protein; CSC, cancer stem cell; DMEM, Dulbecco's modified Eagle's medium; EMT, epithelial-mesenchymal transition; FAK, focal adhesion kinase; FGF, fibroblast growth factor; FN, fibronectin; G, proteoglycan; HS, heparan sulfate; HSPG, heparan sulfate proteoglycan; KLF, Kruppel-like factor; LGR5, leucine-rich repeat containing G protein-coupled receptor 5; MTT, 3-(4,5-dimethylthiazol-2-yl)-2,5-diphenyltetrazolium bromide; RGD, Arg-Gly-Asp; RT-PCR, reverse transcription polymerase chain reaction; SCID, severe combined immunodeficiency; Sdc-1, syndecan-1; siRNA, small-interfering RNA; SOX2, SRY (sex-determining region Y)-box 2; SP, side population; Wnt, wingless-type; ZEB2, zinc finger E-box-binding homeobox 2.

(Received 6 March 2019, revised 23 April 2020, accepted 1 May 2020)

Databases

The GEO accession number of the Affymetrix transcriptomic screening is [GSE58751](#).

doi:10.1111/febs.15356

Introduction

Colorectal cancer is one of the most prevalent cancers [1]. While surgery is the main treatment option, chemo- and radiotherapy are applied in oligometastatic situations and in case of pain due to disseminated decay of critical organs in late stages [2]. However, therapeutic targeting at the metastatic stage is often not successful due to the development of resistance mechanisms, resulting in poor patient survival [3]. Therapeutic resistance and recurrence have been linked to the existence of cancer stem cells (CSCs), aka tumor-initiating cells [4,5]. Cell tracing and lineage tracking studies support the view that malignancies originate from this small-cell population with increased tumor-seeding ability and high therapeutic resistance [4]. CSCs express high levels of multidrug resistance proteins capable of pumping chemotherapeutics out of the cell and show a more efficient DNA repair and detoxification system, which within may account for increased resistance against radiation therapy [5]. Colon cancer is one of the best-studied models to understand CSC characteristics, due to the presence of active stem cells (SCs) at the intestinal crypts, and the high regenerative capacity of the colonic epithelium [6]. At the molecular level, deregulation of the AKT/protein kinase-BK, wingless-type (Wnt), and/or bone morphogenic protein signaling pathways aberrantly affects intestinal stem cell self-renewal [7]. A single stem cell positive for the Wnt target gene leucine-rich repeat containing G protein-coupled receptor 5 (Lgr5) can form a long-lived, self-renewing ‘short minimal-gut’ [8], whereas cells characterized by coexpression of CD133+ and Msi1+ have the highest metastatic ability compared to other marker combinations [9]. High expression of ATP-binding cassette subfamily G member 2 and aldehyde dehydrogenase (ALDH)1 is additional established CSC markers [5,7]. Recent findings in breast cancer have indicated a novel and important role for the transmembrane heparan sulfate (HS) proteoglycan syndecan-1 (Sdc-1) as a modulator of CSC function [10]. The heparin-related HS carbohydrate chains that are attached to the extracellular domain of Sdc-1 are involved in the maintenance of pluripotency and differentiation, enhancing signaling of FGF-2,

BMP4, and Wnt [11–13]. Moreover, during the transition of undifferentiated ESCs into neurally differentiated cells a strong increase in the expression of HS biosynthetic enzymes is observed [14], indicating a role for HS in lineage-specific differentiation.

Sdc-1 binds to a variety of pathophysiologically relevant ligands, including growth factors and morphogens (FGFs, Wnt, BMPs), chemokines, receptor tyrosine kinases, matrix metalloproteinases, integrins, and diverse extracellular matrix substrates [15,16]. Through these interactions, Sdc-1 modulates (tumor) angiogenesis, recruitment of inflammatory cells, (tumor) cell proliferation, cell motility, chemotaxis, and invasiveness [17–19]. Sdc-1 represents the predominant epithelial HS proteoglycan, preserves intestinal structural integrity, and exerts a protective function during colitis [19]. Notably, there is a gradual decrease in Sdc-1 expression from well differentiated to poorly differentiated colon carcinoma and an inverse correlation with patient survival, underscoring its clinicopathological relevance for colon cancer progression [20–22].

Although modulation of a CSC phenotype by Sdc-1 may be of particular relevance for therapeutic resistance, its role in colon CSCs has not been elucidated, yet. In this study, we combine an *in vitro* small-interfering RNA (siRNA) knockdown approach with phenotypic marker analysis, transcriptomic analyses, and *in vivo* xenograft studies to characterize the role of Sdc-1 in CSC function. Our findings indicate that reduced Sdc-1 expression cooperatively enhances activation of integrins, focal adhesion kinase (FAK), and Wnt signaling. Activation of these pathways then generates signals for increased invasiveness and CSC properties of colon cancer cells, with implications for resistance to chemo- and radiotherapy.

Results

Silencing of syndecan-1 enhances the cancer stem cell phenotype in human colon cancer cell lines

To characterize a potential role for Sdc-1 in human colon CSCs, we performed a siRNA knockdown in

Caco2 and HT-29 cells, followed by analysis of established CSC markers [23–26] (Fig. 1A–C). Sdc-1 protein expression was substantially downregulated for at least 14 days (Fig. 1B,C), whereas qPCR analysis revealed no compensatory upregulation of other syndecan family members in Sdc-1-silenced Caco2 cells (Fig. 1D). Compared to controls, Sdc-1-silenced cells showed an increase in the side population (SP), in ALDH1 activity and CD133 expression (Fig. 1E–G), as determined by flow cytometry. Annexin V and propidium iodide (PI) stainings of control and Sdc-1-depleted SP and non-SP cells suggested that the increased SP was not due to an altered cell death rate in the Sdc-1-depleted non-SP (Fig. 1H). Sdc-1 depletion was associated with significantly increased mRNA expression of the stem cell and colon carcinogenesis-related factors *CD133*, *EPCAM*, *LGR5*, *KLF2*, *SOX2*, and *NANOG* (Fig. 2A).

Sdc-1 levels regulate self-renewal and tumorigenicity of colon CSCs

The formation of tumorspheres is a key characteristic of both normal SCs and CSCs, for instance, when transplanted into mice, or placed into 3D Matrigel tissue culture conditions, they recapitulate the cellular architecture, composition, and behavior of tumors *in vivo* [27,28]. Sdc-1-silenced cells showed increased viability and higher ability to form spheres in serum-free suspension cultures (Fig. 2B–E). *In vivo*, Sdc-1-depleted HT-29 cells generated substantially earlier and larger tumors compared to controls when injected subcutaneously into NOD/severe combined immunodeficiency (SCID) mice in two independent experiments (Fig. 3A,B). The tumors in both groups did not reveal obvious differences in the cellular composition based on histology (Fig. 3C,D). Proliferating cell nuclear antigen (PCNA) and PI staining did not indicate differences in apoptosis or proliferation; however, immunohistochemistry revealed a significant downregulation of Sdc-1 protein expression in Sdc-1-silenced tumors harvested after 46 days compared to controls (Fig. 3C–F). In breast cancer cells, Sdc-1 downregulation is associated with increased activation of FAK and altered interactions with fibronectin (FN) [29]. Consistent with these findings, an upregulation of the activated form of FAK and of FN was observed in Sdc-1-deficient tumors (Fig. 3D,G–H). Moreover, upregulation of the pluripotency-associated transcription factor nanog (Fig. 2A) could be confirmed *in vivo* (Fig. 3D,G–I).

Sdc-1 silencing has an impact on the canonical Wnt signaling pathway

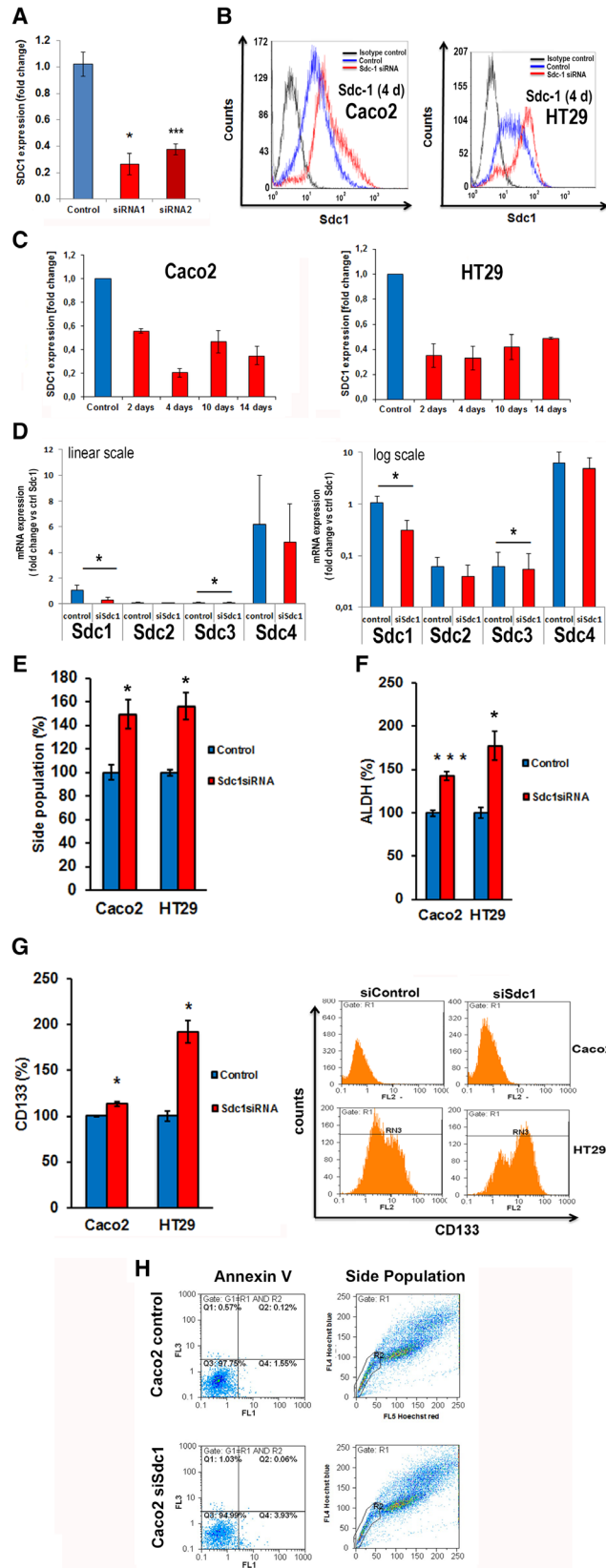
Canonical Wnt signaling is an important gatekeeping pathway in the regulation of CSC properties, which is influenced by HS and HSPGs [10,30–33]. Expression of the Wnt effector TCF7L2 [34] was significantly increased at the mRNA (Fig. 4A) and protein level (Fig. 4B) in Sdc-1-depleted cells. TOPFLASH assay revealed increased TCF/LEF-1 transcriptional activity upon Sdc-1 silencing in Caco2 and HT-29 cells (Fig. 4C). In HT-29 cells, Wnt-1 stimulation increased the control cell SP, whereas the SP of Sdc-1-depleted cells showed an even further increase (Fig. 4D). In contrast, the Wnt inhibitor IWP-2 [35] abolished the SP increase caused by Sdc-1 knockdown in both model cell lines (Fig. 4D).

Sdc-1 knockdown enhances invasive growth and induces an EMT-like phenotype

As Sdc-1 knockdown substantially increased invasiveness of Caco2 cells in Matrigel chambers compared to controls (Fig. 4E), we studied a potential influence of Sdc-1-associated signaling pathways on epithelial-to-mesenchymal transition (EMT) [36–39]. Sdc-1 depletion was associated with decreased expression of E-cadherin and upregulation of the mesenchymal markers Vimentin, FN, and ZEB2 (Fig. 4F,G). Expression of the EMT regulator miR-200b [38] was significantly downregulated in Sdc-1-depleted Caco2 cells (Fig. 4G). Mechanistic inhibitor studies revealed that the FAK inhibitor PF-562271 [40] reduced invasive growth in both control and Sdc-1-depleted Caco2 cells, and significantly reduced the Sdc-1-dependent Vimentin and ZEB2 expression to control levels (Fig. 4E,H). Moreover, Wnt inhibition by IWP-2 and interference with integrin–FN interactions with Arg–Gly–Asp (RGD) peptides reduced the increased invasiveness of Sdc-1-depleted Caco2 cells to control levels (Fig. 4E). While the Wnt inhibitor significantly reduced Vimentin and ZEB2 expression in Sdc-1-depleted cells, RGD peptide treatment resulted in reduced ZEB2 expression in both control and Sdc-1-silenced cells (Fig. 4H).

Sdc-1 depletion results in increased activation of integrin signaling

To understand the molecular pathways by which Sdc-1 depletion mediates an invasive CSC phenotype, we performed a transcriptomic Affymetrix microarray analysis. Twenty-two genes were significantly



upregulated and 48 genes downregulated in Sdc-1-depleted Caco2 cells at least 1.5-fold (Fig. 5A, Table S3). Based on Gene Ontology annotations (Fig. 5B, Table S4), genes involved in cell adhesion, cell motility, and integrin-mediated signaling were differentially regulated with enhancement of the stem cell phenotype (Fig. 5B,C), in accordance with a role of integrin–matrix interactions in CSC function [39]. By qPCR, we could independently confirm upregulation of *ITGA2*, FN, and the RhoA modulator *ARHGAP28* in Sdc-1-depleted cells (Fig. 5C). Upregulation of FN and nanog was also observed in Sdc-1-depleted HT-29 xenografts (Fig. 3D). The retinoic acid-inducible orphan receptor GPRC5A/RAI3 is upregulated in colon cancer [41] and was dysregulated upon Sdc-1 knockdown according to our screening. *GPRC5A* siRNA knockdown significantly reduced the impact of Sdc-1 knockdown on cell viability (Fig. 5D). Importantly, flow cytometric analysis revealed higher activated β 1-integrin levels upon Sdc-1 depletion (Fig. 5E). Phosphorylation of FAK, a kinase acting downstream of β 1-integrin, was increased in Sdc-1-depleted Caco2 (Fig. 5F) and HT-29 (Fig. 5G) cells, as well as in HT-29 xenografts (Fig. 3D). Heparinase treatment also increased FAK activation, suggesting a potential role of cell surface HS in this process (Fig. 5H). Adhesion of Sdc-1-depleted cells to FN was significantly increased compared to controls (Fig. 5I). Pretreatment of the cells with RGD peptide containing the integrin binding site of FN abolished this effect, demonstrating the

importance of increased β 1-integrin activation for Sdc-1-modulated cell adhesion.

Increased FAK phosphorylation in Sdc-1-depleted cells is mechanically related to the augmented CSC phenotype

β 1-integrin and FAK signaling have been linked to EMT- and stemness-related functions in colon cancer and additional tumor entities [42–44]. We hypothesized that increased FAK phosphorylation may be mechanically linked to the augmented stem cell phenotype in Sdc-1-depleted cells. The FAK inhibitor PF-562271 [40] lowered the increased expression of TCF7L2/Tcf-4 at the mRNA and protein levels in Sdc-1-depleted Caco2 cells compared to controls (Fig. 6A,B), abolished the increased SP (Fig. 6C) and ALDH1 activity (Fig. 6D), and lowered the increased expression levels of LGR5, EPCAM, CD133, and NANOG seen in Sdc-1-depleted Caco2 cells to control levels (Fig. 6E). Finally, FAK inhibition significantly reduced the increased sphere formation capacity of Sdc-1-depleted Caco2 cells (Fig. 6F,G).

Sdc-1 siRNA knockdown modulates the CSC phenotype and response to chemotherapy and irradiation

To investigate a potential link of the enhanced stem cell phenotype to radioresistance [45], we irradiated Sdc-1-depleted and control cells with a therapeutically

Fig. 1. Sdc-1 siRNA knockdown enhances the stem cell phenotype in colon cancer cells. (A) qPCR confirmation of Sdc-1 knockdown. Caco2 cells were transfected with Sdc-1 siRNA1, Sdc-1 siRNA2, or negative control siRNA, followed by RNA preparation, and reverse transcription polymerase chain reaction (RT-PCR) 48 h after transfection. Sdc-1 expression is significantly downregulated by both siRNAs ($n = 3$, error bars = SD, $*P < 0.05$, Mann–Whitney U -test). (B,C) Flow cytometric evaluation of Sdc-1 expression following transient Sdc-1 siRNA knockdown in a time course of 0–14 days (siRNA1). siRNA-treated Caco2 and HT-29 cells were analyzed by flow cytometry at the indicated timepoints. Sdc-1 expression is substantially downregulated for at least 14 days. Panel C) shows quantitative evaluation (mean \pm SD) of two independent experiments; panel B) shows a representative analysis performed 4 days after siRNA transfection. (D) qPCR expression analysis of the four members of the syndecan family in Caco2 cells subjected to control or Sdc-1 siRNA treatment (siRNA1, $n = 3$, error bars = SD, $*P < 0.05$, Student's t -test). Expression analysis was performed 48 h after transfection. Among the four syndecans, syndecan-4 is most highly expressed, followed by Sdc-1 expression. Syndecan-2 and syndecan-3 show only negligible expression levels in Caco2 cells (about 6% of the Sdc-1 expression level). Sdc-1 siRNA knockdown results in a significant 70% downregulation of Sdc-1 mRNA expression. Sdc-3 expression is downregulated from 6% to 5% of Sdc-1 expression levels after Sdc-1 knockdown, whereas no compensatory upregulation is observed for any member of the syndecan family. (E–G) Quantitative analysis revealed a 49.6% and 56% increase of SP (E), 42.6% and 77.5% increase of ALDH1 activity (F), and a 3.8% and 92% increase of CD133 expression (G) in Caco2 and HT-29, respectively, upon Sdc-1 knockdown compared to the controls (siRNA1). Data are expressed as mean percentage \pm SEM relative to controls (set to 100%) ($n = 5$ [Caco2], $n = 3$ [HT-29], $*P < 0.05$, $***P < 0.001$, Mann–Whitney U -test). (H) Sdc-1-depleted Caco2 cells display similar apoptosis rates in the SP and non-SP population. Caco2 cells were subjected to Sdc-1 siRNA knockdown (siRNA1) followed by flow cytometric analysis 72 h after transfection. SP analysis was combined with the apoptosis marker Annexin V and PI staining. Sdc-1 knockdown did not induce apoptosis and did not increase cell death, suggesting that the enhanced SP in siSdc-1 Caco2 cells was not a consequence of cells dying of apoptosis rather than a shift in the cellular phenotype. Representative picture of one of two independent experiments. FL1 = Annexin V; FL3 = PI; FL4 = Hoechst blue; FL5 = Hoechst red.

relevant dose of 2 Gy. In Caco2 cells, irradiation increased the control cell SP, whereas Sdc-1 knockdown increased the SP even further (Fig. 7A). qPCR revealed an impact of irradiation on *LGR5* expression in control cells and a substantial increase in Sdc-1-depleted cells. *EPCAM* expression was significantly upregulated in Sdc-1-depleted cells under irradiation, whereas *NANOG* and *KLF2* expression was not substantially altered by irradiation (Fig. 7B). Colony formation assays of Sdc-1-depleted cells revealed an increased survival compared to controls. While the relative survival advantage of Sdc-1-depleted cells was preserved under irradiation conditions, survival was reduced to a similar extent in control and Sdc-1 siRNA knockdown Caco2 cells (Fig. 7C). In contrast, Sdc-1-depleted HT-29 cells showed increased resistance to irradiation compared to controls (Fig. 7C). As stemness has been linked to increased resistance to

chemotherapy [46], we tested its impact on the viability of Sdc-1-depleted HT-29 cells. While Sdc-1 siRNA treatment did not alter sensitivity to cisplatin (results not shown), we observed an increased resistance to doxorubicin (Fig. 7D). However, while the mean viability was higher in Sdc-1-depleted cells over a range of 100 nM–25 μM, the data were only statistically significant for two of the tested concentrations (100 nM, 1 μM), due to a high degree of variability.

SP enrichment enhances the impact of Sdc-1 depletion on the CSC phenotype

Sphere formation in serum-free culture conditions, in addition to allowing quantitative measurements of the number of CSCs present between different assay conditions, is also a model for maintaining CSCs *ex situ*. MammoCult™ is the most published commercially

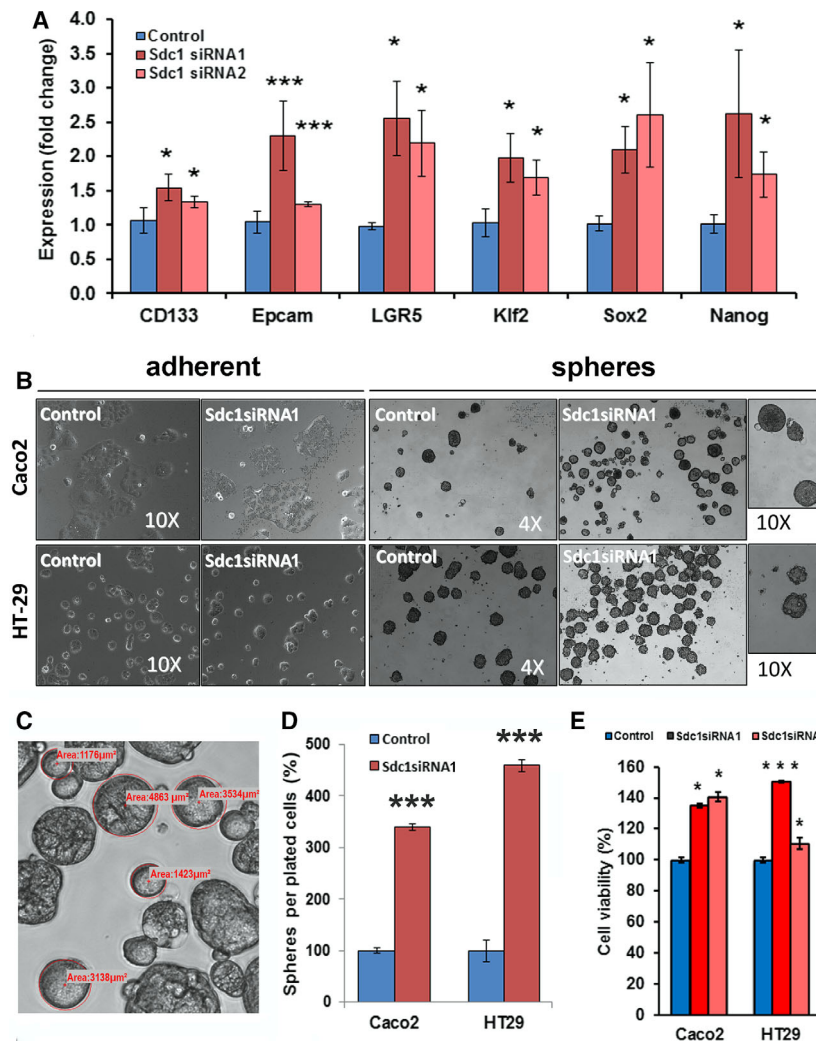
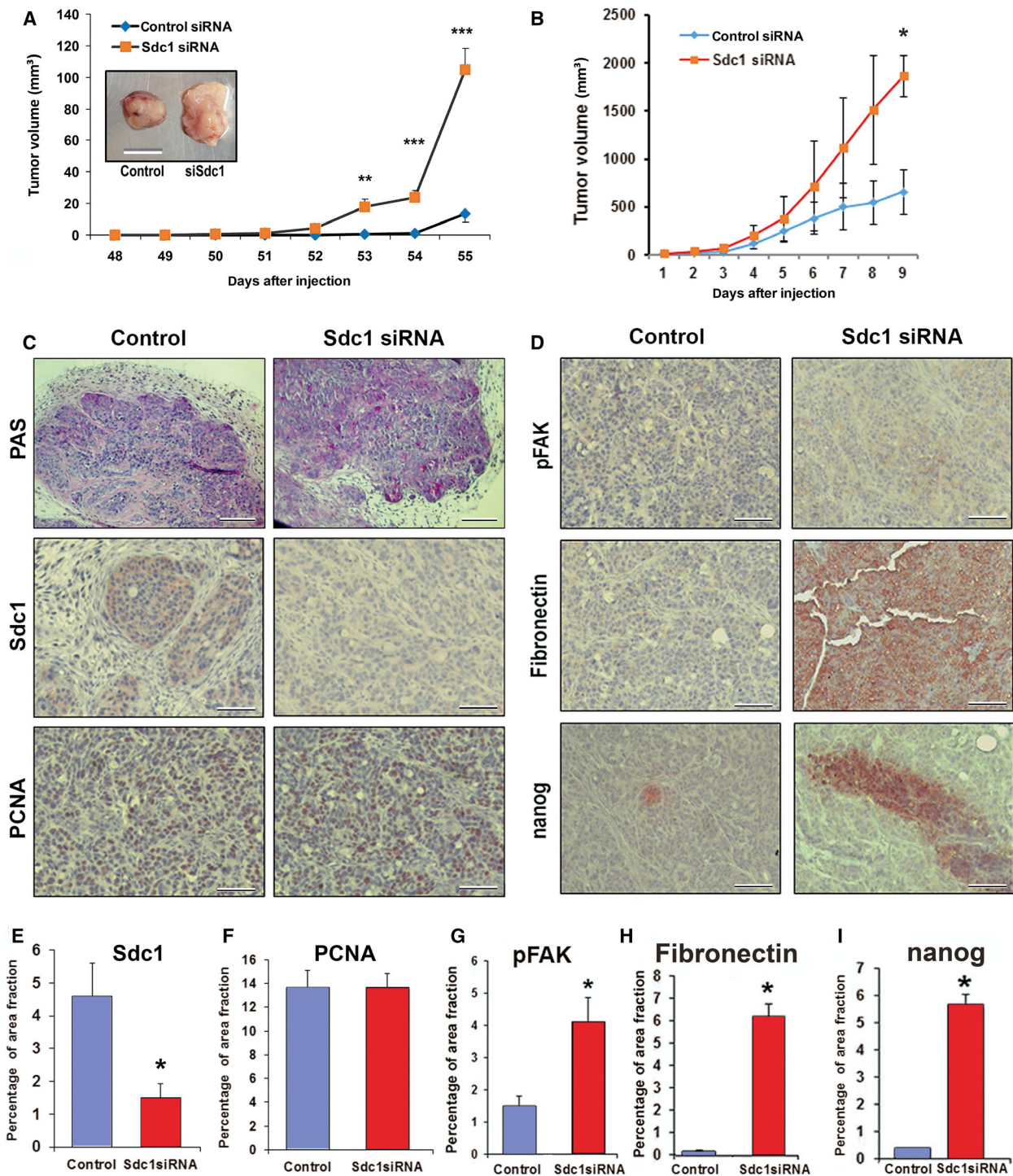


Fig. 2. Sdc-1 siRNA knockdown enhances the expression of stemness-related genes and enhances sphere formation. (A) qPCR analysis of pluripotency-associated genes in Sdc-1-silenced Caco2 cells. Data are expressed as mean percentage ± SEM relative to controls (set to 100%) ($n = 5$ (siRNA1); $n = 3$ (siRNA2), $*P < 0.05$, $***P < 0.001$, Mann–Whitney U -test). (B) Cells were transfected with a control siRNA or Sdc-1 siRNA1, and then cultured in sphere forming culture conditions followed by sphere enrichment. After 1 week, more and larger spheres were formed by Sdc-1 siRNA-transfected Caco2 and HT-29 cells compared to controls (central panel 4×; insert panels 10×). Spheres of a size larger than 60 cells were used for counting to calculate the percentage of spheres formed per number of plated cells. Representative pictures of one of six independent experiments. Quantification is shown in D). (C) Representative pictures of sphere diameters of one of six independent experiments, as quantitatively analyzed in D). (D) Quantitative analysis reveals that Sdc-1 siRNA treatment results in a significant increase of sphere formation efficiency ($***P < 0.001$, $n = 6$, Student’s t -test). (E) Quantitative analysis of cell viability, as determined by MTT. Data are expressed as mean percentage ± SEM relative to the controls (set to 100%) ($n = 13$, $*P < 0.05$, $***P < 0.001$, Student’s t -test).



available medium for the culture of tumorspheres from multiple tissues, including colon [47]. To demonstrate that downregulation of Sdc-1 promotes CSC

properties also in CSC-compatible adherent culture conditions, control and Sdc-1 siRNA-treated Caco2 cells were SP-enriched and grown in adherent culture

Fig. 3. Sdc-1 silencing promotes tumor growth *in vivo*. (A) Increased growth of Sdc-1 siRNA (#1)-transfected vs control siRNA-transfected HT-29 cells in a xenograft mouse model. Three mice per group were injected with 1.0×10^5 cells, and tumor growth was monitored by caliper measurements over a period of 55 days. Sdc-1 siRNA knockdown resulted in a significant increase in tumor volume compared to controls ($n = 3$, $**P < 0.01$, $***P < 0.001$, error bars = SD, Mann–Whitney *U*-test). Insert: representative tumors; scale bar = 1 cm. (B) Independent xenograft cohort experiment. Three mice per group were injected with 1.0×10^5 cells, and tumor growth was monitored by caliper measurements over a period of 46 days. Sdc-1 siRNA (#1) knockdown resulted in a significant increase in tumor volume compared to controls ($n = 3$, $*P < 0.05$, error bars = SEM, Mann–Whitney *U*-test). (C,D) (Immu)histology of xenograft tumor sections. Xenograft tumor tissue from three independent tumor samples was harvested 46 days after injection (2nd mouse group), and formalin-fixed paraffin-embedded tissue sections were processed for periodic acid–Schiff (PAS) staining, or immunostaining for Sdc-1, PCNA, pFAK, FN, or nanog, respectively. Original magnification: 200 \times (PAS), 320 \times (other panels) scale bar = 100 μ m. Representative pictures of samples quantitatively analyzed in (E–I). (E–I) NIH IMAGEJ (NIH, Bethesda MD, USA) based quantitative analysis of immunohistochemistry [4] reveals a significant downregulation of Sdc-1 expression in xenograft tumors, (E), no difference in cell proliferation rates (PCNA) (F), and a significant increase in pFAK (G), FN (H), and nanog (I) expression. Data represent the mean \pm SD of 10 visual fields inspected at 100 \times magnification. $*P < 0.05$, Mann–Whitney *U*-test.

conditions with MammoCult™ serum-free medium. A significant increase in the SP levels and CD133 expression was detected in Sdc-1-depleted cells, whereas the increase in ALDH activity was not statistically significant ($P = 0.13$) (Fig. 8A). We observed an increase in the ability of the Sdc-1-depleted sorted cells to form tumourspheres when grown in suspension culture (Fig. 8B,C) indicating increased self-renewal. Cells from both the adherent colony and sphere assays (Fig. 8B) showed morphological differences compared to those in which a non-SP-enriched pool of Caco2 cells were used (Fig. 2B). Primarily, in adherent tissue culture conditions, colonies from SP-enriched pool of cells appeared more homogenous, having a more round shape and bright and sharper defined colony edges, suggesting a denser cell configuration [28,42,48]. In 3D suspension culture conditions, spheres appeared

more uniformly dense (opaque) and uniform in size and morphology. When cultured in MammoCult media under adherent conditions, Sdc-1-depleted SP-sorted cells showed increased pFAK (Fig. 8D) and TCF4 (Fig. 8E) expression compared to SP control cells. Compared to controls, colony formation in irradiated SP-sorted cells was increased upon Sdc-1 siRNA knockdown, indicating that Sdc-1 depletion renders SP-enriched cells more radioresistant (Fig. 8F).

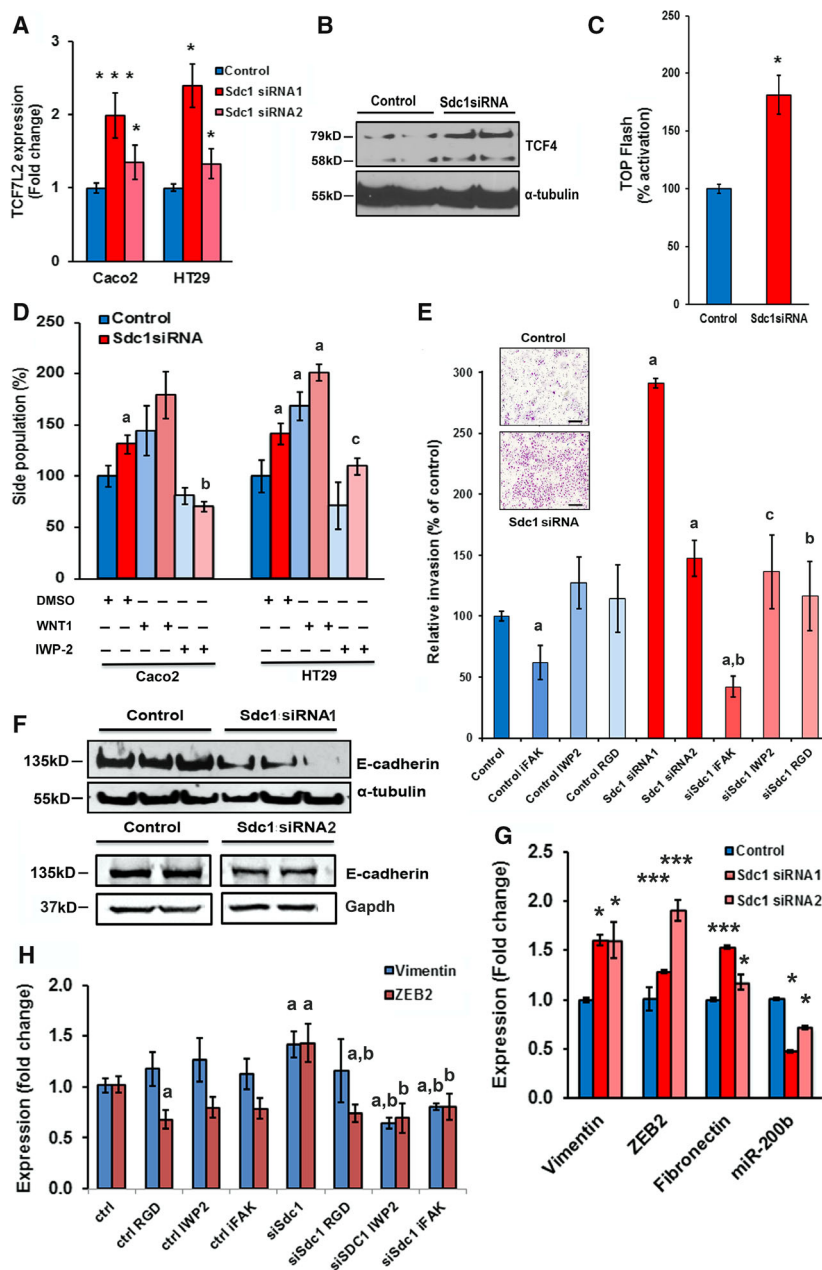
Discussion

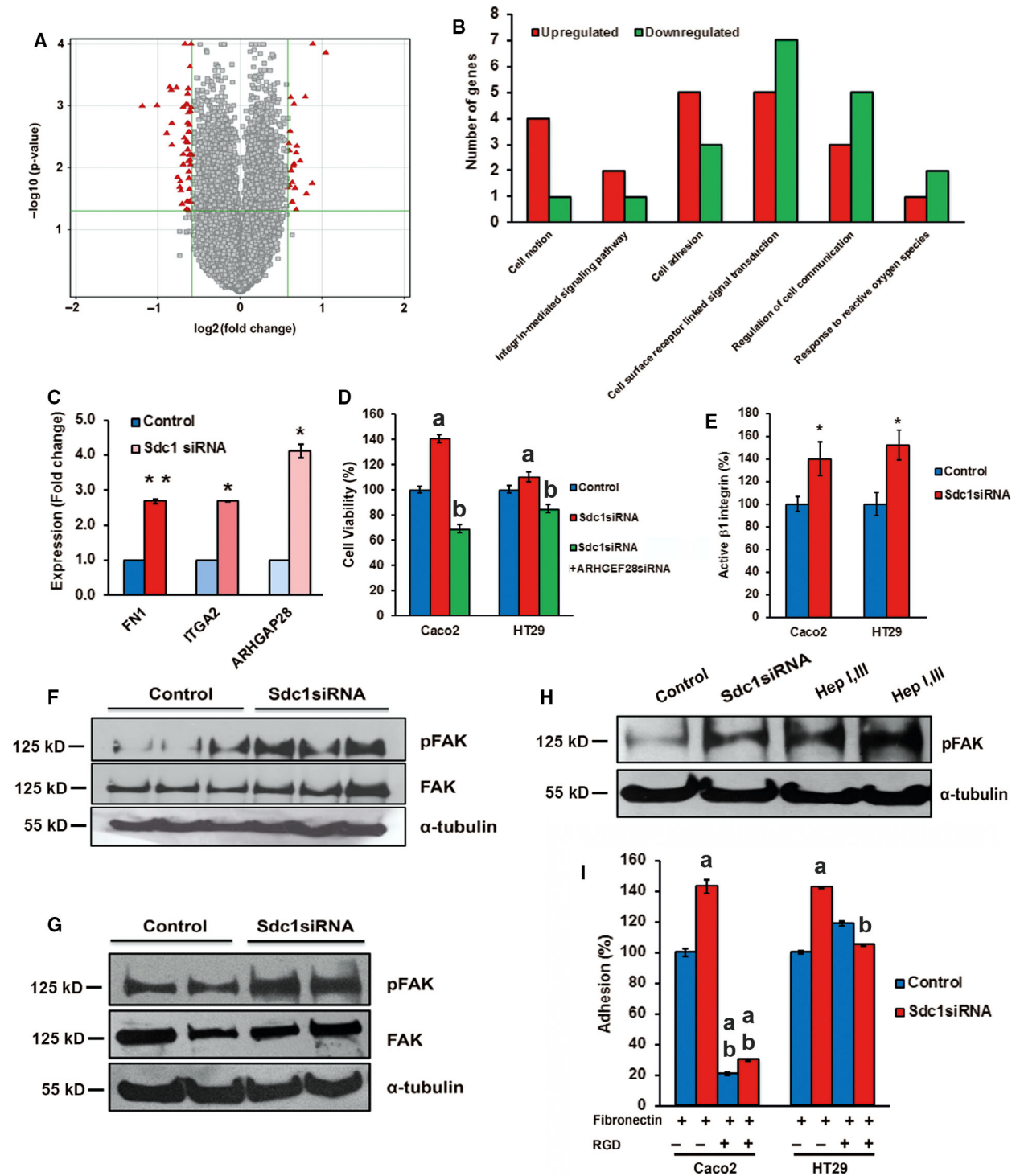
In this study, we demonstrate a novel function of the heparan sulfate proteoglycan (HSPG) Sdc-1 as a regulator of a colon CSC phenotype. While some aspects such as changes in cell viability could be functionally linked to lesser known factors such as GPRC5A

Fig. 4. Sdc-1 siRNA depletion modulates EMT and the activity of the Wnt pathway. (A) qPCR shows 2.5-fold increased TCF7L2 expression in Sdc-1-depleted cells compared to controls. $***P < 0.001$, $*P > 0.05$, $n \geq 3$, error bars = SEM, Mann–Whitney *U*-test. (B) Representative western blot of 4 independent experiments showing increased expression of Tcf7l2/Tcf4 in Caco2 upon Sdc-1 knockdown compared to controls. (C) β -catenin/Tcf-dependent transcriptional activity is increased by 80% in Sdc-1 (#1)-silenced Caco2 cells as determined by TOPFLASH assay. $*P < 0.05$, $n \geq 4$, error bars = SEM, Mann–Whitney *U*-test. (D) Stimulation with Wnt1 ligand for 1 h induces a $\sim 40\%$ and $\sim 20\%$ increase in the SP pool in Sdc-1 (#1)-depleted Caco2 and HT-29 cells, respectively, compared to controls. The Wnt inhibitor IWP-2 abolishes the Sdc-1-dependent increase in the SP. One-way ANOVA: *P*-value 0.0038. Group comparisons (Student's *t*-test): a = $P < 0.05$ compared to DMSO control, b = $P < 0.01$ compared to DMSO/ Sdc-1 siRNA, c = $P < 0.01$ compared to Wnt1/Sdc-1 siRNA, $n \geq 3$, error bars = SEM. (E) Sdc-1 knockdown increases Matrigel invasion in a FAK-, Wnt-, and integrin-dependent manner. Sdc-1-depleted and control Caco2 cells were subjected to a Matrigel invasion chamber assay in the presence or absence of $10 \mu\text{g}\cdot\text{mL}^{-1}$ FAK inhibitor (iFAK) PF-573228, $100 \mu\text{g}\cdot\text{mL}^{-1}$ RGD peptide, or $10 \mu\text{M}$ IWP-2, respectively. While FAK inhibition reduced invasiveness in the control and Sdc-1 knockdown groups, Wnt and integrin inhibition reduced increased invasiveness of Sdc-1-depleted cells. Error bars = SEM, $N = 4$ ANOVA: $P = 0.00858$. Group comparisons (Student's *t*-test): a = $P < 0.05$ vs control; b = $P < 0.05$ vs inhibitor; c = $P = 0.05$ vs inhibitor. Insert = representative images of stained Matrigel matrix filters. Scale bar = 100 μ m. $t = 72$ h. (F) Western blot reveals decreased E-cadherin expression upon Sdc-1 knockdown compared to controls. Representative western blots of three independent experiments. (G) qPCR analysis in Sdc-1-silenced cells indicates a significant change in expression of EMT-regulatory genes compared to control. $N = 9$, error bars = SEM, $*P < 0.05$, $***P < 0.001$ (Student's *t*-test). (H) Sdc-1-dependent upregulation of Vimentin and ZEB2 depends on integrin/FAK and Wnt signaling. Cells were treated as described in (E) and processed for qPCR analysis. ANOVA: $P = 0.00118$. Group comparisons (Student's *t*-test): a = $P < 0.05$ vs untreated control; b = $P < 0.05$ vs inhibitor.

(Fig. 5D) [41], two major signaling pathways appear to be closely linked to the Sdc-1-dependent enhancement of the CSC phenotype, namely Wnt signaling and enhanced integrin/FAK activation. Moreover, pharmacological inhibition of these pathways reduced the increased invasiveness of Sdc-1-depleted cells, partially by reverting the expression of EMT-related gene products (Fig. 4H). Canonical Wnt signaling is an important gate keeping pathway in the regulation of

CSC function in colon cancer [31,49], which induces a reprogramming event that promotes invasion and metastasis [31,36,49]. Cells with the highest Wnt activity were found to define colon CSCs [45], whereas single Lgr5-positive SCs were capable of building crypt-villus structures *in vitro* even in the absence of a mesenchymal niche [1]. The Wnt/ β -catenin pathway regulates growth and maintenance of colonospheres [50], and inhibition of the Wnt signaling pathway via β -





catenin silencing decreases the chemotherapy-resistant colon cancer SP [51]. Data from model organisms indicate an important role for HS in this pathway, and

HSPG of the syndecan and glypican families acts as Wnt coreceptors [13,52,53]. However, their individual roles are context-dependent: Data from Sdc-1-deficient

Fig. 5. siRNA knockdown of Sdc-1 results in activation and upregulation of integrin-associated pathways. (A–C) Affymetrix microarray analysis of control and Sdc-1 siRNA1-transfected Caco2 cells. (A) Volcano plot of genes with at least a twofold change in expression levels with FDR (Benjamin–Hochberg) $P < 0.05$ (red triangles). (B) Number of genes found differentially expressed defined by relevant phenotypic function (Gene Ontology grouping). (C) qPCR confirmation of differential *ITGA2*, *FN1*, and *ARHGAP28* gene expression. $*P < 0.05$, $**P < 0.01$, $n = 9$, error bar = SEM, Student's *t*-test. (D) MTT assay. GPRC5A siRNA knockdown abolishes the increased cell viability caused by Sdc-1 siRNA1 knockdown. ANOVA: P -value = 0.00001. Group comparisons (Student's *t*-test): a = $P < 0.05$ vs untreated control; b = $P < 0.05$ vs Sdc-1 siRNA and control; $n = 3$, error bar = SEM. (E) Flow cytometric analysis reveals a 40% and 50% increase of active $\beta 1$ -integrin expression in Sdc-1-depleted Caco2 and HT-29 cells, respectively, compared to controls. siRNA1, $n = 3$, error bar = SEM, $*P < 0.05$. Student's *t*-test. (F,G) Western blot analysis shows increased FAK phosphorylation upon Sdc-1 siRNA1 knockdown in Caco2 (F) and HT-29 (G) cell lines. (F,G) Representative blot of 3 independent experiments. (H) Heparinase I and III treatment induces increased FAK phosphorylation in Caco2 (representative western blot of three independent experiments) I) Cell adhesion to FN is significantly increased upon Sdc-1 silencing (siRNA1). Interference with integrin–FN interactions by RGD peptide results strongly inhibits adhesion. ANOVA: $P = 0.000001$. Group comparisons (Student's *t*-test): a = $P < 0.05$ vs untreated control; b = $P < 0.05$ vs RGD treatment. $n = 18$, error bars = SEM.

mice suggest that this proteoglycan is required to maintain a Wnt-responsive mammary progenitor cell population [32,53], whereas Sdc-1-deficient mice formed larger tumors compared to controls in a model of colitis-associated colon carcinogenesis, conform with our findings [54]. Syndecan-4 inhibits Wnt/beta-catenin signaling through regulation of LRP6 and R-spondin 3 in mammalian cell lines and *Xenopus* embryos [33]. Moreover, shedding of Sdc-1 in cancer cells can switch syndecan-dependent signaling responses to members of the glypican family [55]. Finally, specific alterations in HS sulfation patterns induce an upregulation of *TCF4/TCF7L2*, with a resulting change in proliferation and invasiveness of cancer cells [30]. While all of these results underscore the importance of Sdc-1 in Wnt signaling in an oncological context, our data indicate that downregulation of colon cancer cell-autonomous Sdc-1 enhances Wnt signaling. This finding may be at least partially due to upregulation of the Wnt coreceptor LGR5, resulting in

enhanced Tcf4 activation. Moreover, the increased SP in Sdc-1-depleted cells would apparently be associated with a relative increase in Wnt signaling in the overall cell population.

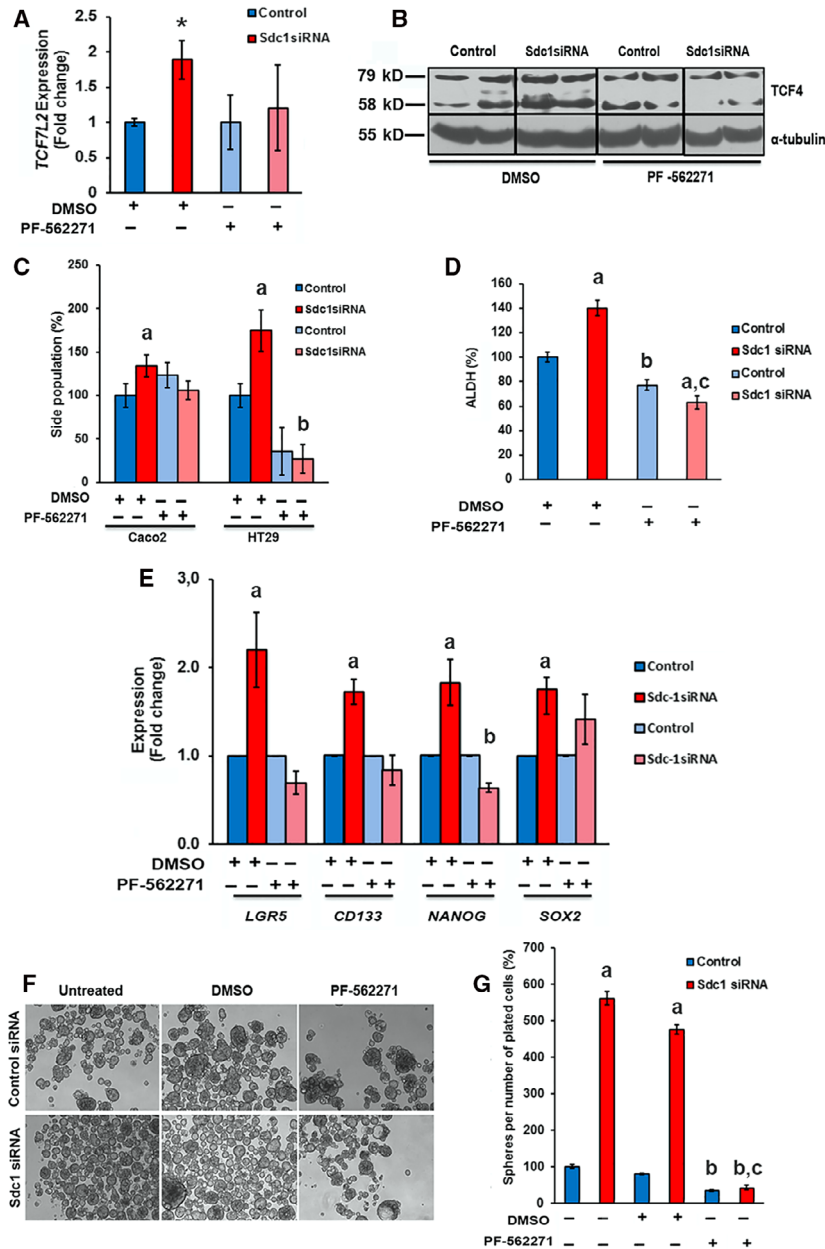
Apart from Wnt signaling, we detected enhanced integrin activity in Sdc-1-depleted colon cancer cells, which was due to increased gene expression (*ITGA2*) and activation ($\beta 1$ -integrin), respectively. *Itga2* enhances the metastatic activity of colon cancer cells [56], and *PHLDA1*, a candidate human intestinal epithelial stem cell marker, is regulated by *ITGA2* levels [57]. In association with the $\beta 1$ -subunit, $\alpha 2$ -integrin increases tumorigenicity and loss of the differentiated epithelial phenotype in colon cancer [58]. Particularly, $\beta 1$ -integrins are key regulators of proliferation and homeostasis in the intestine, which influence signaling pathways relevant to stem cell function [59], and promote metastatic behavior in colon cancer cells [60]. Interestingly, Tcf4, which was dysregulated in our experimental system upon Sdc-1 siRNA knockdown,

Fig. 6. Impact of Sdc-1-dependent FAK activation on the stem cell phenotype. (A, B) Pharmacological inhibition of FAK reduces Sdc-1-dependent upregulation of *TCF4/TCF7L2* in Caco2. (A) qPCR analysis of *TCF7L2* expression in control and Sdc-1 siRNA1-depleted cells treated with or without $10 \mu\text{g}\cdot\text{mL}^{-1}$ of the FAK inhibitor PF-573228 (1 h). ANOVA $P = 0.01225$. Group comparison (Student's *t*-test): $*P < 0.05$ vs control, $n = 9$, error bar = SEM. (B) Western blot analysis of Tcf7l2 expression after 2 h of treatment with $10 \mu\text{g}\cdot\text{mL}^{-1}$ PF-573228. Representative blot of 3 independent experiments. (C–H) Treatment with $10 \mu\text{g}\cdot\text{mL}^{-1}$ of PF-573228 for 1 h decreases the CSC phenotype. FAK inhibition decreases the Sdc-1 siRNA1 knockdown-dependent increase in (C) the SP ($N = 3$, ANOVA $P = 0.00017$, group comparison (Student's *t*-test): a = $P < 0.05$ vs control; b = $P < 0.05$ vs inhibitor; error bars = SEM), and (D) ALDH activity (Caco2, $n = 3$, ANOVA $P = 0.0001$, group comparisons (Student's *t*-test): a = $P < 0.001$ vs control; b = $P < 0.05$ vs control; c = $P < 0.001$ vs siSdc-1. error bars = SEM). (E) qPCR analysis reveals that increased mRNA expression of LGR5, CD133, NANOG, and SOX2 in Sdc-1-deficient Caco2 cells is abolished by FAK inhibition. ANOVA $P = 0.001$, group comparisons (Student's *t*-test): a = $P < 0.05$ vs control; b = $P > 0.05$ vs siSdc-1 (siRNA1). $n = 3$, error bars = SEM. (F,G) FAK inhibition abolishes the Sdc-1-dependent increase in Caco2 sphere forming capacity. Representative micrograph of 3 independent experiments (F, see Fig. 2C for diameters) and quantitative analysis (G) of sphere formation \pm Sdc-1 siRNA knockdown \pm FAK inhibitor treatment. Sdc-1 siRNA1 knockdown results in a significant ~ 5 fold increase compared to controls, while FAK inhibition suppresses sphere formation in both controls and Sdc-1-depleted cells. ANOVA $P = 0.00001$, group comparisons (Student's *t*-test): a = $P < 0.001$ vs control; b = $P < 0.001$ vs inhibition; c = $P < 0.05$ inhibited control vs siSdc-1, $n = 3$, error bars = SEM.

mislocalizes in the intestinal epithelia of $\beta 1$ integrin-deleted mice [59], suggesting a crosstalk of the two major signaling pathways affected by Sdc-1 depletion. The demonstration that E-cadherin, which was dysregulated upon Sdc-1 depletion, acts as an integrin ligand further supports this view [61]. Finally, enhanced expression of the integrin- and HS-ligand FN in Sdc-1-depleted Caco2 cells may have enhanced signaling via these pathways, enhancing both cell motility and stem cell properties.

An important downstream signal transducer of integrin signaling is FAK, previously shown to co-

immunoprecipitate with Sdc-1 [18]. Consistent with increased integrin activation, FAK phosphorylation was enhanced upon Sdc-1 depletion in Caco2 cells. While our finding of increased FAK activation upon degradation of cell surface HS further supports a role for cell surface HSPG in this pathway, it has to be considered that not only Sdc-1, but also other cell surface HSPGs, such as Sdc-4 or glypicans, could have contributed to this effect [13]. For example, Sdc-2 was shown to regulate FAK activity in HT-29 cells depending on phosphorylation of the variable region of its cytoplasmic domain [62].



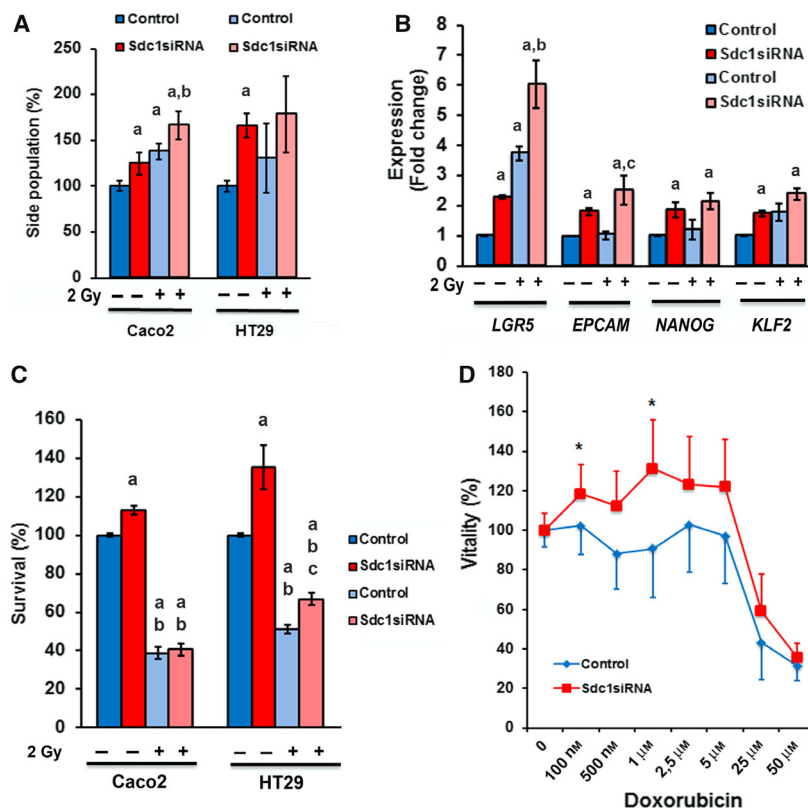


Fig. 7. Sdc-1 depletion modulates changes in the colon CSC pool in response to irradiation and doxorubicin chemotherapy. (A–C) Control and Sdc-1 siRNA1-transfected cells were subjected to irradiation with 2 Gy. (A) After 4 h of radiation, the SP was analyzed by flow cytometry. In Caco2 cells, irradiation induced an increase of the SP. ANOVA $P = 0.00186$. Group comparisons (Student's t -test): $a = P < 0.05$ vs untreated control; $b = P < 0.05$ nonirradiated vs irradiated. ($n = 3$). (B) Radiation treatment induces significant increases in the expression of the stem cell markers LGR5 and EPCAM in Sdc-1-depleted Caco2 cells, as assessed by RT-PCR ANOVA: $P < 0.04$. Group comparisons (Student's t -test): $a = P < 0.05$ vs untreated control; $b = P < 0.05$ irradiated vs nonirradiated; $c = P < 0.05$ irradiated control vs siSdc-1 (siRNA1), ($n = 3$). (C) Colony survival assay shows an increase in the basal survival rate upon Sdc-1 siRNA1 knockdown in Caco2 and HT-29. Depletion of Sdc-1 increases radiation resistance in HT-29 cells. ANOVA: $P = 0.00001$. Group comparisons (Student's t -test): $a = P < 0.001$ vs untreated control; $b = P < 0.001$ irradiated vs nonirradiated; $c = P < 0.001$ irradiated control vs irradiated siSdc-1, ($n = 6$). (D) Sdc-1 siRNA1-depleted HT-29 cells show increased resistance to doxorubicin treatment in MTT cell viability assays ($n = 5$, $*P < 0.05$, Mann-Whitney U -test). (A–D) Error bars = SEM.

Our finding of a novel link between Sdc-1 and FAK activation is of clinicopathological relevance, as FAK is overexpressed in colon cancer [63]. FAK inhibition blocked several of the Sdc-1-related phenotypic changes, suggesting that increased FAK activation may be a pivotal point in the Sdc-1-dependent signaling network. Notably, these changes are probably not only linked to enhanced invasive behavior and resistance to radiation (see Ref. [29] for discussion), but also to the CSC phenotype: FAK was shown to be linked to the Wnt pathway and to regulate intestinal regeneration and tumorigenesis, altering the response to radiotherapy [64]. Finally, downregulation of FAK activity decreases transcription of the Wnt (co)receptors Frizzled and LRP5 and increases transcription of the Wnt inhibitor,

Dickkopf-1, demonstrating that FAK acts upstream of the Wnt pathway in colon cancer [65].

Conclusions

In summary, we have demonstrated a novel role for the HSPG Sdc-1 as a regulator of a colon CSC phenotype. Mechanistically, Sdc-1 depletion is associated with increased activation of integrins, HS-dependent downstream activation of FAK signaling, and activation of the Wnt/Tcf4 signaling pathway. The activation of these pathways promotes an EMT-like process, which promotes tumor cell viability and tumor growth *in vivo*, invasive growth, and increased resistance to chemo- and radiation therapy. We provide novel

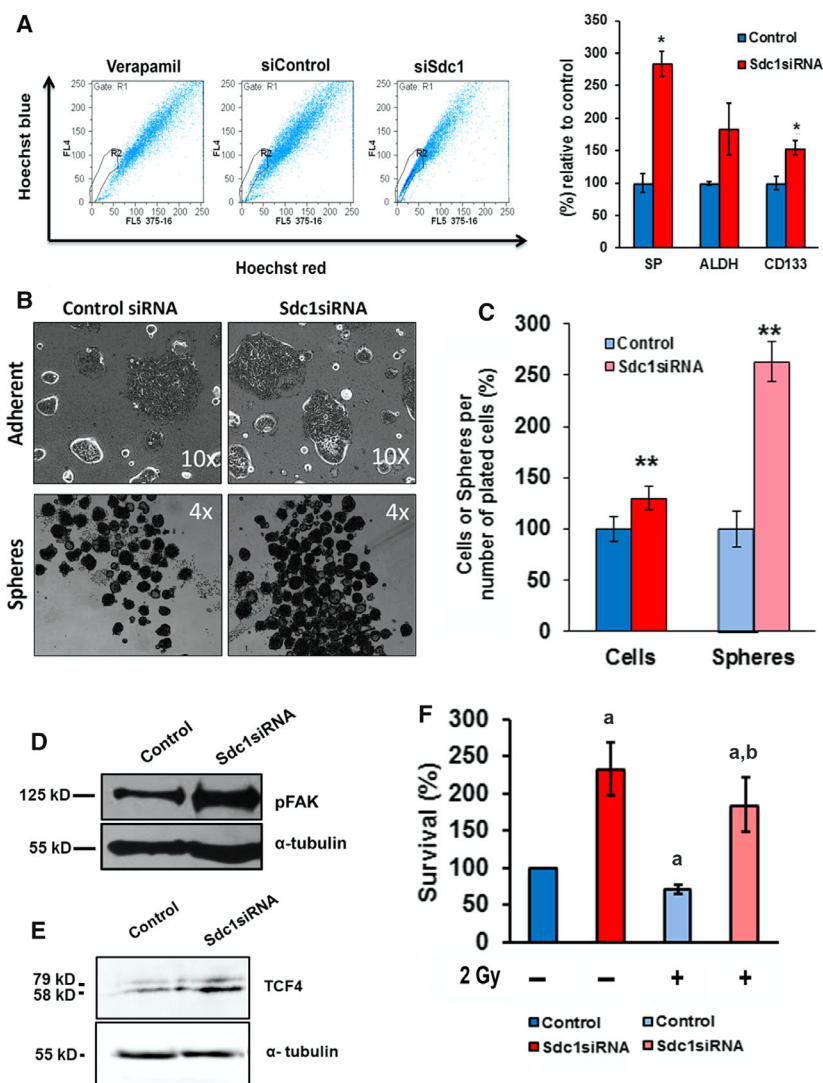


Fig. 8. SP enrichment and culturing in MammoCult media enhance the stem cell phenotype of Sdc-1-silenced Caco2 cells. The SP of control siRNA or Sdc-1 siRNA1-treated cells was isolated by flow cytometric sorting, cultured in MammoCult (adherent) or sphere media, and re-analyzed for stemness-associated parameters. (A) Sdc-1-depleted cells cultured in MammoCult show a significant ~ 3 fold increase in the SP. ALDH activity was nonsignificantly increased ($P = 0.13$), whereas CD133 expression was significantly increased by 38% upon Sdc-1 depletion. $*P < 0.05$, $n = 3$, error bars = SEM (Mann–Whitney U -test). Left panel = representative picture of SP analysis; right panel = quantitative analysis. (B, C) Sdc-1-depleted SP -enriched cells show increased cell numbers/plated cell in MammoCult media, and increased sphere numbers when cultured in sphere media. (B) Morphology of cells cultured in MammoCult or sphere media, respectively. Representative picture from three independent experiments. (C) Quantitative analysis. $**P < 0.01$, $n = 3$, error bars = SEM, Student's t -test. (D-E) Increased expression of pFAK and Tcf4 in SP-enriched Sdc-1-depleted cells cultured in MammoCult media. Representative western blots of two independent experiments. (F) Sdc-1-depleted SP-enriched cells cultured in MammoCult media show a substantial increase in the colony survival rate, with an increased survival rate after irradiation compared to controls (compare with Fig. 7D). Data are expressed as mean percentage \pm SEM relative to controls (set to 100%). ANOVA: $P = 0.00014$. Group comparisons (Student's t -test): a = $P < 0.01$ vs untreated control; b = $P < 0.05$ irradiated control vs irradiated siSdc-1 ($n = 3$).

evidence that Sdc-1 levels regulate self-renewal of colon CSCs. In particular, we show that modulation of levels of Sdc-1 alone is sufficient to promote loss of colon CSC self-renewal, suggesting that Sdc-1 is a key

player maintaining the CSC pool. We conclude that interference with Sdc-1-dependent signaling processes emerges as a promising approach in the therapeutic targeting of colon cancer.

Materials and methods

Antibodies and reagents

Antibodies are listed in Table S1. GRGDSP peptide was from Calbiochem (EMD Biosciences Inc. La Jolla, CA, USA). Wnt1 was from PeproTech (Hamburg, Germany). Unless stated otherwise, FAK inhibitor (PF-573228), IWP-2, heparinase I/III, and all additional chemicals were from Sigma (Deisenhofen, Germany), and all media, FBS, and tissue culture supplies were from Gibco BRL (Karlsruhe, Germany).

Adherent cell culture

The human colon cancer cell lines Caco2 and HT-29, authenticated by STR analysis, were provided by the German Collection of Microorganisms and Cell Cultures, Braunschweig, Germany. Cells were routinely tested for the absence of mycoplasma contaminations using the Venor GeM Classic Kit (Minerva Biolabs, Berlin, Germany). Cells were maintained with RPMI-1640 (Caco2) or Dulbecco's modified Eagle's medium (DMEM) (HT-29) supplemented with 10% (v/v) FBS and 1% (v/v) penicillin/streptomycin in a humidified atmosphere of 5% and 7% CO₂ at 37 °C. Cells were cultured to 80% confluence. In some experiments, cell surface HS was degraded by adding 0.5 U·mL⁻¹ of heparinase I and III to the culture medium for 3 h as described [66].

siRNA knockdown

siRNA knockdown was performed using siRNAs silencer select #s12634 ('siRNA 1') and silencer #12527 ('siRNA 2') (Ambion, Cambridgeshire, UK) targeting the coding region (border of exons 2 and 3, location bp 452, and exon 5, location bp 1222, accession no. NM_002997.4, respectively) of Sdc-1, siRNA #17259 (Ambion) targeting the coding region of GPCR5A, and a negative control siRNA (negative control #1; Ambion). Cells were serum starved for 5 h before transfection at 50–70% confluence using 40 nM siRNA and DharmaFECT reagent (Dharmacon, Lafayette, CO, USA) according to the manufacturer's instructions. Fresh medium was added 16 h after transfection, and experiments were conducted 48 h after transfection. Target downregulation was confirmed by qPCR (Fig. 1A).

Enrichment of Caco2 and HT-29 cells with sphere formation capacity

Enrichment of spheres

Colonospheres are a model for culturing and maintaining colon SCs or CSCs *ex situ*. Spheres are generated from single CSCs as previously described culture and characterization of mammary CSCs in mammospheres [67,68]. Caco2

sphere cultures were generated by plating single cells in low attachment plates (Corning, Kaiserslautern, Germany) at 1000 cells per mL into RPMI-1640 supplemented with B-27 (Life Technologies, Wesel, Germany), 25 ng·mL⁻¹ basic fibroblast growth factor (bFGF; Sigma-Aldrich), 20 ng·mL⁻¹ mouse recombinant EGF (Sigma-Aldrich), and 4 ng·mL⁻¹ heparin (Sigma-Aldrich) ('Sphere media'). HT-29 sphere cultures were generated analogously using DMEM supplemented with 5% FBS B-27, 25 ng·mL⁻¹ bFGF, 20 ng·mL⁻¹ mouse recombinant EGF, and 4 ng·mL⁻¹ heparin [68].

Sdc-1 silencing in sphere cultures

A total of 9500 cells were plated in 24-well plates under adherent conditions 48 h before the treatment. Cells were transfected with 50 nM Sdc-1 siRNA1 (#12634; Ambion) or negative control siRNA (Ambion), using INTERFERIN® (Polyplus-transfection, Illkirch-Graffenstaden, France) according to the manufacturer's instructions. Twenty-four hours later, cells were washed, trypsinized (0.25% trypsin/EDTA; Gibco, Life Technologies), counted, and seeded in suspension culture. Fresh sphere medium was added every 3 days. Caco2 and HT-29 spheres were counted after 7 and 11 days.

FAK inhibitor treatment

siRNA-transfected Caco2 cells were seeded at 20 000 cells per cm². After 24 h, the medium was changed and cells were treated with either the inhibitor PF-562271 (10 µg·mL⁻¹) or vehicle as control (0.05% DMSO). After 48 h, cells were washed, trypsinized, counted, and plated as single cells in sphere medium containing the same inhibitor or DMSO, respectively. Media were replaced after 3 days, and spheres were counted after 7 and 11 days from suspension plating.

SP enrichment using flow cytometry

5 × 10⁶ cells were transfected with control siRNA and Sdc-1 siRNA 2 (#12527; Ambion). After 72 h, cells were subjected to sort SP cells from control and Sdc siRNA cells a CyFlow Space flow cytometer (Sysmex Partec, Münster, Germany). These cells were maintained for 5 days in adherent culture conditions with MammoCult serum-free media. Further, these cultured cells were used for SP, CD133, ALDH levels (by FACS), colony formation ability, western blot, and sphere formation ability as described in the respective methods sections.

Cell viability and chemosensitivity assay

Cell viability [18] and chemosensitivity in the presence of doxorubicin hydrochloride (100 nM–50 µM) [36] were

evaluated by 3-(4,5-dimethylthiazol-2-yl)-2,5-diphenyltetrazolium bromide (MTT) assay as previously described [17,36].

Cell adhesion assay

A cell adhesion assay based on the photometric detection of borate-buffered (pH 8.5) methylene blue staining of cells bound to different substrates was performed as described [29], using 96-well plates coated with 50 $\mu\text{g}\cdot\text{mL}^{-1}$ FN, 100 $\mu\text{g}\cdot\text{mL}^{-1}$ GRGDSP peptide, or 10 $\mu\text{g}\cdot\text{mL}^{-1}$ BSA as a negative control.

Invasion assay

BioCoat Matrigel Invasion Chamber (BD Biosciences, Heidelberg, Germany) assay was performed exactly as described [18].

Quantitative real-time PCR (qPCR)

Total cellular RNA was isolated using RNA-OLS (OMNI Life Science, Hamburg, Germany) and reverse-transcribed (Advantage First-strand cDNA Synthesis Kit; Fermentas, St. Leon-Rot, Germany). qPCR and melting curve analysis were performed using either Qiagen QuantiTect SYBR Green PCR Kit (Qiagen, Hilden, Germany) in a LightCycler (Roche, Mannheim, Germany), or TaqMan probes on an ABI PRISM 7300 Sequence Detection System [18]. The $2^{-\Delta\Delta C_t}$ method was used to determine relative gene transcript levels after normalization to 18S rRNA. Primers are listed in Table S2.

Immunoblot

Immunoblotting was performed as described [2] using 30–60 μg of protein/lane on 5–7.5% gels. Antibodies are listed in Table S1.

TOPFLASH/FOPFLASH reporter assay

Twenty-four hours after siRNA transfection, cells were cultured in serum-containing media for 6 h and cotransfected with 1 μg of plasmid/well (6-well) TOPFLASH/FOPFLASH luciferase reporters [Addgene, Cambridge, MA, USA, plasmid #12456 and 12457, [69] using FuGENE 6 Reagent (Promega, Mannheim, Germany)] according to the manufacturer's instructions. Per well, 0.5 ng Renilla control luciferase plasmid was cotransfected to normalize for transfection efficiency. Forty-six hours after transfection, cells were lysed, and luciferase activity was assayed in a luminometer using the Dual-Luciferase Reporter Assay Kit (GeneCopoeia, Rockville, MD, USA). TOPFLASH and FOPFLASH values were normalized to Renilla activity,

and fold induction was calculated as TOPFLASH/FOPFLASH signal ratio.

Affymetrix microarray expression analysis

Total RNA was isolated from three biological replicates of scrambled siRNA control and Sdc-1 siRNA-transfected cells using the basic RNA-OLS Kit (OLS, Bremen, Germany). Preparation of biotin-labeled cRNA using the 1-cycle labeling protocol, hybridization, and scanning of the arrays was performed as described [18]. 3.6 μg of purified RNA and poly-A controls were used to generate cDNA, which was used to synthesize biotin-labeled cRNA. Fragmented cRNA was hybridized to Human Genome U133 Plus 2.0 Arrays for 16 h at 60 °C in a GeneChip Hybridization Oven 640 at 60 r.p.m. The arrays were washed and stained in a GeneChip Fluidics 450 station (Affymetrix, Singapore, Singapore), followed by scanning (Affymetrix GeneChip Scanner 3000). The raw data image was processed with GENECHIP OPERATING Software v1.2 (Affymetrix) and analyzed using GeneSpring GX 11.0 with Robust Multiarray Average normalization. A list of differentially expressed genes was generated using the filtering criteria of $P < 0.05$ after Benjamini–Hochberg false discovery rate control and fold change of at least 2. The DAVID 2008 database was used to verify the annotations of the filtered genes ($n = 396$) and classify them into ontology groups. The GEO accession number of this screening is GSE58751.

Flow cytometry

All flow cytometric analyses were performed on a CyFlow Space flow cytometer (Sysmex Partec). SP analysis was performed 72 h after siRNA transfection using Hoechst 33342 dye exclusion [3]. Apoptosis was evaluated using an Annexin V test kit (Becton Dickinson, San José, CA, USA) as described [70]. When combined, SP staining was done first, followed by CD133 labeling. In stimulation experiments, Wnt1 was used 50 $\text{ng}\cdot\text{mL}^{-1}$ and IWP-2 at 10 μM for 1 h. SP and non-SP cells were sorted by flow cytometry, and SP cells were enriched in adherent conditions using MammoCult media (STEMCELL Technologies, Cologne, Germany) and in suspension conditions using sphere media. ALDH-1 activity was assessed 72 h after siRNA transfection using the ALDEFLUOR™ kit (STEMCELL Technologies) [10,29]. Fluorescence emission was measured at 520 nm in FL1. Gates were set by comparing the fluorescence of the DEAB control with that of the original sample. CD133 was detected using mouse anti-CD133-PE mAb (clone AC133) and IgG1-PE isotype control (Miltenyi Biotec, Bergisch Gladbach, Germany). Ten microlitre of each antibody was given to 1×10^6 cells suspended in 90 μL PBS with 0.1% BSA and incubated for 20 min in

the dark. After final addition of 5 mL PBS/BSA and centrifugation at 400 *g*, cells were resuspended in 1 mL PBS/BSA. Fluorescence emission was detected at 570 nm in FL2 and quantified by setting a region gate. Mouse anti-human-integrin $\beta 1$ mAb HUTS-4 (Millipore, Darmstadt, Germany) was used to analyze the active conformation of $\beta 1$ -integrins. About 1×10^6 cells were incubated with 2.5 μg mAb for 1 h at room temperature. Cells were washed with PBS/BSA and incubated with Alexa 488-conjugated goat anti-mouse secondary antibody (Invitrogen, Karlsruhe, Germany, 1 : 1000) for 30 min at 25 °C in the dark. After a final washing step, fluorescence emission was detected at 520 nm in FL1 and quantified by setting a region gate.

Radiation exposure

Cells were irradiated with 2Gy at room temperature using 6 MV photons of a linear accelerator (Varian Medical Systems, Palo Alto, CA, USA) at a dose rate of 4.8Gy per minute.

Colony forming assay

1×10^3 irradiated or untreated knockdown cells were plated into 3.5-cm petri dishes with a 2.5 mm grid (Nunc, Langensfeld, Germany) and incubated for 8–12 days in a CO₂ incubator at 37 °C. Colonies with more than 50 cells were counted using a microscope (Olympus, Hamburg, Germany). The survival fraction was calculated as plating efficiency treated/plating efficiency control [29].

NOD/SCID mouse xenograft model

In vivo xenograft experiments were approved by the local animal committee 'OMC' [Ospedale San Raffaele Mouse Clinic, San Raffaele, Segrate-Milano, Italy (IACUC #590)] and performed at the DIBIT, Milan, Italy. All experiments were performed in accordance with relevant guidelines and regulations, including implementation of a harm–benefit analysis and the doctrine of replacement, reduction, and refinement. HT-29 cells were plated under adherent conditions 72 h before transfection with INTERFERin® reagent (Polyplus-transfection) and 50 nM Sdc-1 siRNA #12634 (Ambion), or 50 nM negative control #1 (Ambion) according to the manufacturer's instructions. After 48 h, cells were trypsinized, counted, and prepared for injection (0.25% trypsin/EDTA; Gibco, Life Technologies). For each condition, 1.0×10^5 transfected cells were injected subcutaneous in the neck of NSG (NOD scid gamma; Charles River Laboratories Italia, SRL, Sant'Angelo Lodigiano LO, Italy) mice. The mice were anesthetized with isoflurane prior to tumor cell injection. Two independent experiments with three animals/group were performed. Animals were

sacrificed 55 days (exp.1) or 46 days (exp.2) after injection. Tumor size was estimated daily using calipers by measuring the difference in the suspect tumor width, which includes the width of the animal skin, subtracted from width of the folded skin of a control region of the animal. Tumor volume was calculated from the linear dimensions using the formula: Volume = (width)² × length/2 [71]. Immunohistochemical analysis of formalin-fixed, paraffin-embedded xenograft tumor sections was performed exactly as described previously [3], employing the DAKO EnVision + Dual Link System-horseradish peroxidase (DAB+) Kit (DAKO, Glostrup, Denmark). Primary antibodies are listed in Table S1. Quantitative analysis of immunohistochemical staining results was performed on 10 visual fields at 100× magnification using NIH IMAGEJ software as previously described [72].

Statistics

Unless stated otherwise, all experiments were repeated at least three times in triplicates. Data are presented as mean values ± SEM. In case two or more treatment groups were analyzed, data were analyzed by one-way ANOVA. Individual group comparisons were tested for significance employing Student's unpaired *t*-test in case of normally distributed data and Mann–Whitney *U*-test in case of non-normally distributed data. The level of significance was set at $P < 0.05$.

Acknowledgements

The authors would like to acknowledge Birgit Pers and Annette von Dülmen for expert technical assistance, Stefan Schlatt for providing access to histology equipment, and Tomo Saric, Ludwig Kiesel, Rita Dreier, Andreas Ludwig, Michael Elkin, and Israel Vladavsky for discussions and for the generous gift of reagents.

Funding was provided by Deutsche Forschungsgemeinschaft DFG International Research Training Group 'Molecular and Cellular GlycoSciences' Grant GRK 1549 (to SKK, MG), German-Israeli Foundation grant I-1004-202.15/2008 (MG), EU H2020 MSCA-RISE-2014 no. 645756 GLYCANC (MG, SAI), the N.O.B.E.L. Grant and Cariplo Progetti-Internazionali n. 2008-2015 (Fondazione Cariplo) (IZ), MUIR-FIRB (IZ), RBAP11BYNP (IZ), InterOmics Flag Project (IZ), and National Medical Research Council, Singapore Grant NMRC/CSA/0041/2012 (GWY).

Conflict of interest

The authors declare no conflict of interest.

Author contributions

SKK performed most of the experiments, designed experiments, analyzed data, and drafted the manuscript. VT and PP performed sphere formation assays and analyzed data. W-CS performed Affymetrix analysis. GWY designed and analyzed Affymetrix screening and supervised the study. W-CS and SM performed pharmacological inhibitor assays in 3D cultures. TK performed animal experiments. SAI performed *in vitro* cell line studies and designed experiments. EAE performed western blots, flow cytometry, and immunohistology. EP performed *in vitro* cell culture assays and molecular biology. IZ performed xenograft tumor analysis, analyzed data, and supervised the study. VT, SM and RR designed 3D culture studies and supervised the study. VT, SM, EP, and SKK analyzed data and participated in writing the manuscript. BG performed, designed, and supervised flow cytometric analysis. SKK analysed data and co-wrote the manuscript. MG conceived, supervised, and designed the study and co-wrote the manuscript. All authors reviewed the manuscript. The results presented in this study are part of the Ph.D. thesis of Sampath Kumar Katakam at the Faculty of Biology of the University of Münster, Germany (WWU).

References

- Gallagher DJ & Kemeny N (2010) Metastatic colorectal cancer: from improved survival to potential cure. *Oncology* **78**, 237–248.
- Quirke P, West NP & Nagtegaal ID (2014) EURECCA consensus conference highlights about colorectal cancer clinical management: the pathologists expert review. *Virchows Arch* **464**, 129–134.
- Helling TS & Martin M (2014) Cause of death from liver metastases in colorectal cancer. *Ann Surg Oncol* **21**, 501–506.
- Blanpain C (2013) Tracing the cellular origin of cancer. *Nat Cell Biol* **15**, 126–134.
- Greve B, Kelsch R, Spaniol K, Eich HT & Gotte M (2012) Flow cytometry in cancer stem cell analysis and separation. *Cytometry A* **81**, 284–293.
- Barker N, van de Wetering M & Clevers H (2008) The intestinal stem cell. *Genes Dev* **22**, 1856–1864.
- Garza-Trevino EN, Said-Fernandez SL & Martinez-Rodriguez HG (2015) Understanding the colon cancer stem cells and perspectives on treatment. *Cancer Cell Int* **15**, 2.
- Sato T, Vries RG, Snippert HJ, van de Wetering M, Barker N, Stange DE, van Es JH, Abo A, Kujala P, Peters PJ *et al.* (2009) Single Lgr5 stem cells build crypt-villus structures *in vitro* without a mesenchymal niche. *Nature* **459**, 262–265.
- Todaro M, Perez Alea M, Scopelliti A, Medema JP & Stassi G (2008) IL-4-mediated drug resistance in colon cancer stem cells. *Cell Cycle* **7**, 309–713.
- Ibrahim SA, Hassan H, Vilardo L, Kumar SK, Kumar AV, Kelsch R, Schneider C, Kiesel L, Eich HT, Zucchi I *et al.* (2013) Syndecan-1 (CD138) modulates triple-negative breast cancer stem cell properties via regulation of LRP-6 and IL-6-mediated STAT3 signaling. *PLoS ONE* **8**, e85737.
- Lanner F, Lee KL, Sohl M, Holmborn K, Yang H, Wilbertz J, Poellinger L, Rossant J & Farnebo F (2010) Heparan sulfation-dependent fibroblast growth factor signaling maintains embryonic stem cells primed for differentiation in a heterogeneous state. *Stem Cells* **28**, 191–200.
- Fico A, De Chevigny A, Egea J, Bosl MR, Cremer H, Maina F & Dono R (2012) Modulating Glypican4 suppresses tumorigenicity of embryonic stem cells while preserving self-renewal and pluripotency. *Stem Cells* **30**, 1863–1874.
- Vitale D, Kumar Katakam S, Greve B, Jang B, Oh ES, Alaniz L & Götte M (2019) Proteoglycans and glycosaminoglycans as regulators of cancer stem cell function and therapeutic resistance. *FEBS J* **286**, 2870–2882.
- Johnson CE, Crawford BE, Stavridis M, Ten Dam G, Wat AL, Rushton G, Ward CM, Wilson V, van Kuppevelt TH, Esko JD *et al.* (2007) Essential alterations of heparan sulfate during the differentiation of embryonic stem cells to Sox1-enhanced green fluorescent protein-expressing neural progenitor cells. *Stem Cells* **25**, 1913–1823.
- Yip GW, Smollich M & Gotte M (2006) Therapeutic value of glycosaminoglycans in cancer. *Mol Cancer Ther* **5**, 2139–2148.
- Szatmari T, Otvos R, Hjerpe A & Dobra K (2015) Syndecan-1 in cancer: implications for cell signaling, differentiation, and prognostication. *Dis Markers* **2015**, 796052.
- Nikolova V, Koo CY, Ibrahim SA, Wang Z, Spillmann D, Dreier R, Kelsch R, Fischgrabe J, Smollich M, Rossi LH *et al.* (2009) Differential roles for membrane-bound and soluble syndecan-1 (CD138) in breast cancer progression. *Carcinogenesis* **30**, 397–407.
- Ibrahim SA, Yip GW, Stock C, Pan JW, Neubauer C, Poeter M, Pujalis D, Koo CY, Kelsch R, Schule R *et al.* (2012) Targeting of syndecan-1 by microRNA miR-10b promotes breast cancer cell motility and invasiveness via a Rho-GTPase- and E-cadherin-dependent mechanism. *Int J Cancer* **131**, E884–E896.
- Floer M, Gotte M, Wild MK, Heidemann J, Gassar ES, Domschke W, Kiesel L, Luegering A & Kucharzik T (2010) Enoxaparin improves the course of dextran sodium sulfate-induced colitis in syndecan-1-deficient mice. *Am J Pathol* **176**, 146–157.

- 20 Hashimoto Y, Skacel M & Adams JC (2008) Association of loss of epithelial syndecan-1 with stage and local metastasis of colorectal adenocarcinomas: an immunohistochemical study of clinically annotated tumors. *BMC Cancer* **8**, 185.
- 21 Day RM, Hao X, Ilyas M, Daszak P, Talbot IC & Forbes A (1999) Changes in the expression of syndecan-1 in the colorectal adenoma-carcinoma sequence. *Virchows Arch* **434**, 121–125.
- 22 Mennerich D, Vogel A, Klamann I, Dahl E, Lichtner RB, Rosenthal A, Pohlenz HD, Thierauch KH & Sommer A (2004) Shift of syndecan-1 expression from epithelial to stromal cells during progression of solid tumours. *Eur J Cancer* **40**, 1373–1382.
- 23 Haraguchi N, Ohkuma M, Sakashita H, Matsuzaki S, Tanaka F, Mimori K, Kamohara Y, Inoue H & Mori M (2008) CD133+CD44+ population efficiently enriches colon cancer initiating cells. *Ann Surg Oncol* **15**, 2927–2933.
- 24 Huang EH, Hynes MJ, Zhang T, Ginestier C, Dontu G, Appelman H, Fields JZ, Wicha MS & Boman BM (2009) Aldehyde dehydrogenase 1 is a marker for normal and malignant human colonic stem cells (SC) and tracks SC overpopulation during colon tumorigenesis. *Cancer Res* **69**, 3382–3389.
- 25 Hirsch D, Barker N, McNeil N, Hu Y, Camps J, McKinnon K, Clevers H, Ried T & Gaiser T (2014) LGR5 positivity defines stem-like cells in colorectal cancer. *Carcinogenesis* **35**, 849–858.
- 26 Xiong B, Ma L, Hu X, Zhang C & Cheng Y (2014) Characterization of side population cells isolated from the colon cancer cell line SW480. *Int J Oncol* **45**, 1175–1183.
- 27 Pece S, Tosoni D, Confalonieri S, Mazzarol G, Vecchi M, Ronzoni S, Bernard L, Viale G, Pelicci PG & Di Fiore PP (2010) Biological and molecular heterogeneity of breast cancers correlates with their cancer stem cell content. *Cell* **140**, 62–73.
- 28 Zucchi I, Astigiano S, Bertalot G, Sanzone S, Cocola C, Pelucchi P, Bertoli G, Stehling M, Barbieri O, Albertini A *et al.* (2008) Distinct populations of tumor-initiating cells derived from a tumor generated by rat mammary cancer stem cells. *Proc Natl Acad Sci USA* **105**, 16940–16945.
- 29 Hassan H, Greve B, Pavao MS, Kiesel L, Ibrahim SA & Götte M (2013) Syndecan-1 modulates beta-integrin-dependent and interleukin-6-dependent functions in breast cancer cell adhesion, migration, and resistance to irradiation. *FEBS J* **280**, 2216–2227.
- 30 Vijaya Kumar A, Salem Gassar E, Spillmann D, Stock C, Sen YP, Zhang T, Van Kuppevelt TH, Hulsewig C, Koszowski EO, Pavao MS *et al.* (2014) HS3ST2 modulates breast cancer cell invasiveness via MAP kinase- and Tcf4 (Tcf712)-dependent regulation of protease and cadherin expression. *Int J Cancer* **135**, 2579–2592.
- 31 Fevr T, Robine S, Louvard D & Huelsken J (2007) Wnt/beta-catenin is essential for intestinal homeostasis and maintenance of intestinal stem cells. *Mol Cell Biol* **27**, 7551–7559.
- 32 Liu BY, Kim YC, Leatherberry V, Cowin P & Alexander CM (2003) Mammary gland development requires syndecan-1 to create a beta-catenin/TCF-responsive mammary epithelial subpopulation. *Oncogene* **22**, 9243–9253.
- 33 Astudillo P, Carrasco H & Larrain J (2014) Syndecan-4 inhibits Wnt/beta-catenin signaling through regulation of low-density-lipoprotein receptor-related protein (LRP6) and R-spondin 3. *Int J Biochem Cell Biol* **46**, 103–112.
- 34 van Es JH, Haegerbarth A, Kujala P, Itzkovitz S, Koo BK, Boj SF, Korving J, van den Born M, van Oudenaarden A, Robine S *et al.* (2012) A critical role for the Wnt effector Tcf4 in adult intestinal homeostatic self-renewal. *Mol Cell Biol* **32**, 1918–1927.
- 35 Arensman MD, Kovochich AN, Kulikauskas RM, Lay AR, Yang PT, Li X, Donahue T, Major MB, Moon RT, Chien AJ *et al.* (2014) WNT7B mediates autocrine Wnt/beta-catenin signaling and anchorage-independent growth in pancreatic adenocarcinoma. *Oncogene* **33**, 899–908.
- 36 Miyaki M, Tanaka K, Kikuchi-Yanoshita R, Muraoka M, Konishi M & Takeichi M (1995) Increased cell-substratum adhesion, and decreased gelatinase secretion and cell growth, induced by E-cadherin transfection of human colon carcinoma cells. *Oncogene* **11**, 2547–2552.
- 37 Pap Z, Pavai Z, Denes L, Kovalszky I & Jung J (2009) An immunohistochemical study of colon adenomas and carcinomas: E-cadherin, Syndecan-1, Ets-1. *Pathol Oncol Res* **15**, 579–587.
- 38 Eggers JC, Martino V, Reinbold R, Schäfer SD, Kiesel L, Starzinski-Powitz A, Schüring AN, Kemper B, Greve B & Götte M (2016) microRNA miR-200b affects proliferation, invasiveness and stemness of endometriotic cells by targeting ZEB1, ZEB2 and KLF4. *Reprod Biomed Online* **32**, 434–445.
- 39 Farahani E, Patra HK, Jangamreddy JR, Rashedi I, Kawalec M, Rao Pariti RK, Batakis P & Wiechec E (2014) Cell adhesion molecules and their relation to (cancer) cell stemness. *Carcinogenesis* **35**, 747–759.
- 40 Roberts WG, Ung E, Whalen P, Cooper B, Hulford C, Autry C, Richter D, Emerson E, Lin J, Kath J *et al.* (2008) Antitumor activity and pharmacology of a selective focal adhesion kinase inhibitor, PF-562,271. *Cancer Res* **68**, 1935–1944.
- 41 Zougman A, Hutchins GG, Cairns DA, Verghese E, Perry SL, Jayne DG, Selby PJ & Banks RE (2013) Retinoic acid-induced protein 3: identification and

- characterisation of a novel prognostic colon cancer biomarker. *Eur J Cancer* **49**, 531–539.
- 42 Schober M & Fuchs E (2011) Tumor-initiating stem cells of squamous cell carcinomas and their control by TGF- β and integrin/focal adhesion kinase (FAK) signaling. *Proc Natl Acad Sci USA* **108**, 10544–10549.
- 43 Ashton GH, Morton JP, Myant K, Pesse TJ, Ridgway RA, Marsh V, Wilkins JA, Athineos D, Muncan V, Kemp R *et al.* (2010) Focal adhesion kinase is required for intestinal regeneration and tumorigenesis downstream of Wnt/c-Myc signaling. *Dev Cell* **19**, 259–269.
- 44 Tancioni I, Miller NL, Uryu S, Lawson C, Jean C, Chen XL, Kleinschmidt EG & Schlaepfer DD (2015) FAK activity protects nucleostemin in facilitating breast cancer spheroid and tumor growth. *Breast Cancer Res* **17**, 47.
- 45 Ghisolfi L, Keates AC, Hu X, Lee DK & Li CJ (2012) Ionizing radiation induces stemness in cancer cells. *PLoS ONE* **7**, e43628.
- 46 Richard V, Nair MG, Santhosh Kumar TR & Pillai MR (2013) Side population cells as prototype of chemoresistant, tumor-initiating cells. *Biomed Res Int* **2013**, 517237.
- 47 Huang X, Sheng Y & Guan M (2012) Co-expression of stem cell genes CD133 and CD44 in colorectal cancers with early liver metastasis. *Surg Oncol* **21**, 103–107.
- 48 Rowehl RA, Burke S, Bialkowska AB, Pettet DW 3rd, Rowehl L, Li E, Antoniou E, Zhang Y, Bergamaschi R, Shroyer KR *et al.* (2014) Establishment of highly tumorigenic human colorectal cancer cell line (CR4) with properties of putative cancer stem cells. *PLoS ONE* **9**, e99091.
- 49 Vermeulen L, De Sousa EMF, van der Heijden M, Cameron K, de Jong JH, Borovski T, Tuynman JB, Todaro M, Merz C, Rodermond H *et al.* (2010) Wnt activity defines colon cancer stem cells and is regulated by the microenvironment. *Nat Cell Biol* **12**, 468–476.
- 50 Kanwar SS, Yu Y, Nautiyal J, Patel BB & Majumdar AP (2010) The Wnt/beta-catenin pathway regulates growth and maintenance of colonospheres. *Mol Cancer* **9**, 212.
- 51 Chikazawa N, Tanaka H, Tasaka T, Nakamura M, Tanaka M, Onishi H & Katano M (2010) Inhibition of Wnt signaling pathway decreases chemotherapy-resistant side-population colon cancer cells. *Anticancer Res* **30**, 2041–2048.
- 52 Pataki CA, Couchman JR & Brabek J (2015) Wnt signaling cascades and the roles of syndecan proteoglycans. *J Histochem Cytochem* **63**, 465–480.
- 53 Alexander CM, Reichsman F, Hinkes MT, Lincecum J, Becker KA, Cumberledge S & Bernfield M (2000) Syndecan-1 is required for Wnt-1-induced mammary tumorigenesis in mice. *Nat Genet* **25**, 329–332.
- 54 Binder Gallimidi A, Nussbaum G, Hermano E, Weizman B, Meirovitz A, Vlodavsky I, Gotte M & Elkin M (2017) Syndecan-1 deficiency promotes tumor growth in a murine model of colitis-induced colon carcinoma. *PLoS ONE* **12**, e0174343.
- 55 Ding K, Lopez-Burks M, Sanchez-Duran JA, Korc M & Lander AD (2005) Growth factor-induced shedding of syndecan-1 confers glypican-1 dependence on mitogenic responses of cancer cells. *J Cell Biol* **171**, 729–738.
- 56 Ferraro A, Boni T & Pintzas A (2014) EZH2 regulates cofilin activity and colon cancer cell migration by targeting ITGA2 gene. *PLoS ONE* **9**, e115276.
- 57 Sakhthianandeswaren A, Christie M, D'Andreti C, Tsui C, Jorissen RN, Li S, Fleming NI, Gibbs P, Lipton L, Malaterre J *et al.* (2011) PHLDA1 expression marks the putative epithelial stem cells and contributes to intestinal tumorigenesis. *Cancer Res* **71**, 3709–3719.
- 58 Kirkland SC & Ying H (2008) Alpha2beta1 integrin regulates lineage commitment in multipotent human colorectal cancer cells. *J Biol Chem* **283**, 27612–27619.
- 59 Jones RG, Li X, Gray PD, Kuang J, Clayton F, Samowitz WS, Madison BB, Gumucio DL & Kuwada SK (2006) Conditional deletion of beta1 integrins in the intestinal epithelium causes a loss of Hedgehog expression, intestinal hyperplasia, and early postnatal lethality. *J Cell Biol* **175**, 505–514.
- 60 Fujimoto K, Beauchamp RD & Whitehead RH (2002) Identification and isolation of candidate human colonic clonogenic cells based on cell surface integrin expression. *Gastroenterology* **123**, 1941–1948.
- 61 Whittard JD, Craig SE, Mould AP, Koch A, Pertz O, Engel J & Humphries MJ (2002) E-cadherin is a ligand for integrin alpha2beta1. *Matrix Biol* **21**, 525–532.
- 62 Jang B, Jung H, Choi S, Lee YH, Lee ST & Oh ES (2017) Syndecan-2 cytoplasmic domain up-regulates matrix metalloproteinase-7 expression via the protein kinase C γ -mediated FAK/ERK signaling pathway in colon cancer. *J Biol Chem* **292**, 16321–16332.
- 63 Lark AL, Livasy CA, Calvo B, Caskey L, Moore DT, Yang X & Cance WG (2003) Overexpression of focal adhesion kinase in primary colorectal carcinomas and colorectal liver metastases: immunohistochemistry and real-time PCR analyses. *Clin Cancer Res* **9**, 215–222.
- 64 Williams KE, Bundred NJ, Landberg G, Clarke RB & Farnie G (2015) Focal adhesion kinase and Wnt signaling regulate human ductal carcinoma in situ stem cell activity and response to radiotherapy. *Stem Cells* **33**, 327–341.
- 65 Fonar Y, Gutkovich YE, Root H, Malyarova A, Aamar E, Golubovskaya VM, Elias S, Elkouby YM & Frank D (2011) Focal adhesion kinase protein regulates Wnt3a gene expression to control cell fate specification in the developing neural plate. *Mol Biol Cell* **22**, 2409–2421.

- 66 Götte M, Kresse H & Hausser H (1995) Endocytosis of decorin by bovine aortic endothelial cells. *Eur J Cell Biol* **66**, 226–233.
- 67 Piscitelli E, Cocola C, Thaden FR, Pelucchi P, Gray B, Bertalot G, Albertini A, Reinbold R & Zucchi I (2015) Culture and characterization of mammary cancer stem cells in mammospheres. *Methods Mol Biol* **1235**, 243–262.
- 68 Morata-Tarifa C, Jimenez G, Garcia MA, Entrena JM, Grinan-Lison C, Aguilera M, Picon-Ruiz M & Marchal JA (2016) Low adherent cancer cell subpopulations are enriched in tumorigenic and metastatic epithelial-to-mesenchymal transition-induced cancer stem-like cells. *Sci Rep* **6**, 18772.
- 69 Veeman MT, Slusarski DC, Kaykas A, Louie SH & Moon RT (2003) Zebrafish prickles, a modulator of noncanonical Wnt/Fz signaling, regulates gastrulation movements. *Curr Biol* **13**, 680–685.
- 70 Greve B, Sheikh-Mounessi F, Kemper B, Ernst I, Götte M & Eich HT (2012) Survivin, a target to modulate the radiosensitivity of Ewing's sarcoma. *Strahlenther Onkol* **188**, 1038–1047.
- 71 Jacob D, Davis J & Fang B (2004) Xenograftic tumor models in mice for cancer research, a technical review. *Gene Ther Mol Biol* **8**, 213–219.
- 72 Kaczmarek E, Gorna A & Majewski P (2004) Techniques of image analysis for quantitative immunohistochemistry. *Rocz Akad Med Białymst* **49** (Suppl 1), 155–158.

Supporting information

Additional supporting information may be found online in the Supporting Information section at the end of the article.

Table S1. List of antibodies used in this study.

Table S2. List of PCR primers used in this study.

Table S3. Gene expression changes in Sdc-1-siRNA vs control siRNA treated Caco2 cells according to Affymetrix Human Genome U133 plus 2.0 array analysis.

Table S4. Gene expression changes linked to the GO groupings shown in the main manuscript.